Supplemental Information

Inventory of Supplemental Items

- Figure S1-S4
- Supplemental Experimental Procedures
- Supplemental References

Supplemental Figures and Legends

A

Over-Abundant Proteins in Plasma	
Protein	Fold change
Adam10	1.5
Adamts2	1.3
Agt	1.3
Ak1	1.5
Angptl3	1.8
Apcs	2.1
Coro1a	1.3
Eif2ak3	9.0
F7	1.3
Fgfr2	Cancer only
Hamp2	3.1
Igfbp4	1.4
Igsf4a	1.5
Ltbp2	1.4
Lyzs	1.8
Man2b2	1.5
Morc3	10.0
Ncan	1.5
Npc2	3.5
Nup188	Cancer only
Pf4	1.6
Pglyrp1	1.4
Ppbp	1.7
Ppia	1.3
Prtg	10.0
Rarres2	2.5
Sftpb	3.4
Slit2	Cancer only
Son	10.0
Tfpi2	Cancer only
Tspan5	10.0
Vnn3	1.3
Wfdc2	2.3

Under-Abundant Proteins in Plasma	
Protein	Fold change
Arg1	0.1
C1r	0.8
C6	0.2
C8a	0.2
C8b	0.3
C9	0.3
Camta2	0.1
Cand2	0.1
Egfr	0.4
Hamp1	0.3
Hp	0.4
Mug1	0.4
Mup1	0.2
Mup2	0.3
Notch1	0.5
Pam	0.2
Pear1	0.1
Pon1	0.7
Prg4	0.6
Proz	0.8
Rgn	0.2
Sepp1	0.7
Serpina3k	0.6
Smarcc2	0.1
Tfpi	0.5
Thumpd1	0.1
Wdr62	0.4

B

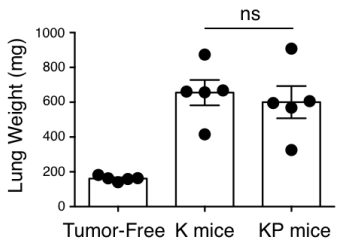

C

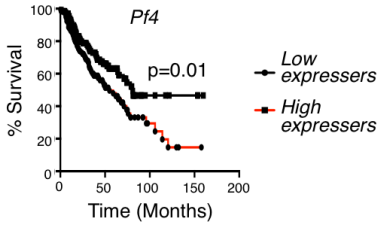

D

Demographic and clinical characteristics of two cohorts of lung cancer patients

Variable	*PF4^{hi}* (n=133)	*PF4^{lo}* (n=133)	P Value
Median age (range) — yr	65.1 (36-87)	64.4 (33-89)	0.563
Male sex — %	53	45	0.270
Smoking history — Cases			0.636
Currently smoking	9	11	
Never smoked	69	70	
Smoked in the past	16	10	
Unknown	39	42	
Histologic grade — Cases			0.890
Well differentiated	9	11	
Moderate differentiation	28	31	
Poorly differentiated	32	28	
Unknown	64	63	
Stage — Cases			0.298
IA	31	45	
IB	51	52	
IIA	4	5	
IIB	3	2	
IIIA/B	26	16	
IIIC/IV	18	13	
Adjuvant chemotherapy — Cases			0.325
No	47	47	
Yes	72	64	
Unknown	14	22	
Adjuvant radiation therapy — Cases			0.586
No	50	55	
Yes	72	64	
Unknown	11	14	
EGFR mutation — Cases			0.544
Unknown	108	108	
Ex19	4	1	
Ex21	2	0	
L858R	0	2	
Negative	19	22	
KRAS mutation — Cases			0.949
Unknown	108	108	
G12A	0	1	
G12C	2	2	
G12D	3	0	
G12V	1	3	
G13C	0	1	
Negative	19	18	

Figure S1. Related to Figure 1. Identification of candidate long-range factors associated with altered survival in lung adenocarcinoma.

(**A**) Plasma proteins over- or under-abundant in lung adenocarcinoma murine models as previously published (Taguchi et al., 2011).

(**B**) Lung weight as proxy for tumor burden in mice used for gene expression analysis in Figure 1D-E.

(**C**) Kaplan-Meier survival curves for patients with highest (top 20%, n = 133) and lowest (bottom 20%, n = 133) mRNA expression levels for *Pf4*. Data are from 4 additional datasets (Nguyen et al., 2009).

(**D**) Contingency table comparing clinical covariates corresponding to the pooled top 20% highest *PF4* expressers (*PF4^{HI}*) and bottom 20% lowest *PF4* expressers (*PF4^{LO}*). Data were associated to the microarray datasets used for survival analysis presented in Fig 1B-C and S1B-C. Median age is shown in years (yr) and all other variables are presented as number of patients for each cohort (*PF4^{HI}* or *PF4^{LO}*). Unpaired 2-tailed Student's t test was performed to compare age groups. Fisher's exact test or chi-squared test were performed to compare frequency distributions. *p < 0.05. Abbreviations are as follows: K, *Kras^{G12D}*; KP, *Kras^{G12D};p53$^{fl/fl}$*; ns, not significant.

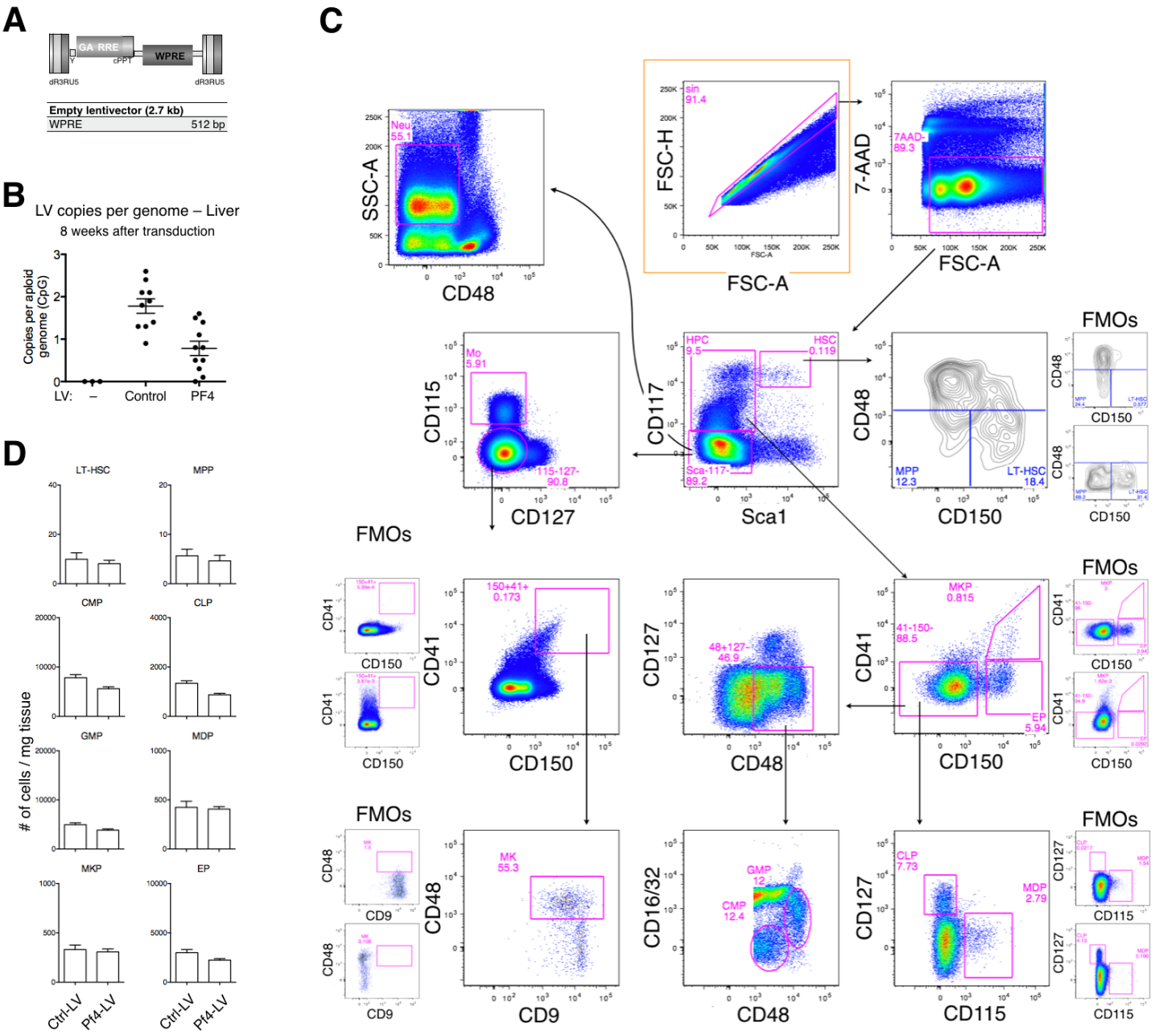

Figure S2. Related to Figure 2. Study of BM and spleen hemopoiesis after systemic PF4 over-expression in K mice

(**A**) Features of Ctrl-LV. Ctrl-LV is "empty" since it does not contains an expression cassette.

(**B**) Analysis of LV copy number in liver from mice treated with the indicated LV eight weeks earlier. Each dot corresponds to one mouse.

(**C**) Gating strategy used to quantify bone marrow and spleen cell subsets in Fig 2E-F. Orange outline define initial ungated plot. Sequential gating on regions is indicated by arrows. FMO (fluorescence minus one) controls are on the side of relevant plots.

(**D**) Flow cytometry-based analysis of splenic hemopoietic stem/progenitor cells from mice treated as in Fig. 2C.

Abbreviations are as follows: CLP, common lymphoid progenitors; CMP, common myeloid progenitors; Ctrl-LV, Control lentivector; EP, erythroid progenitors; FMO, fluorescence minus one; GMP, granulocyte-macrophage progenitors; LT-HSC, long-term hemopoietic stem cells; HPC, hemopoietic progenitor cells; MDP, monocyte-dendritic cell progenitors; MK, megakaryocyte; MKP, megakaryocyte progenitors; Mo, monocytes; MPP, multi-potent progenitors; Neu, neutrophils; Pf4-LV, Pf4 lentivector; sin, singlets; WPRE, Woodchuck hepatitis virus Post-transcriptional Regulatory Element.

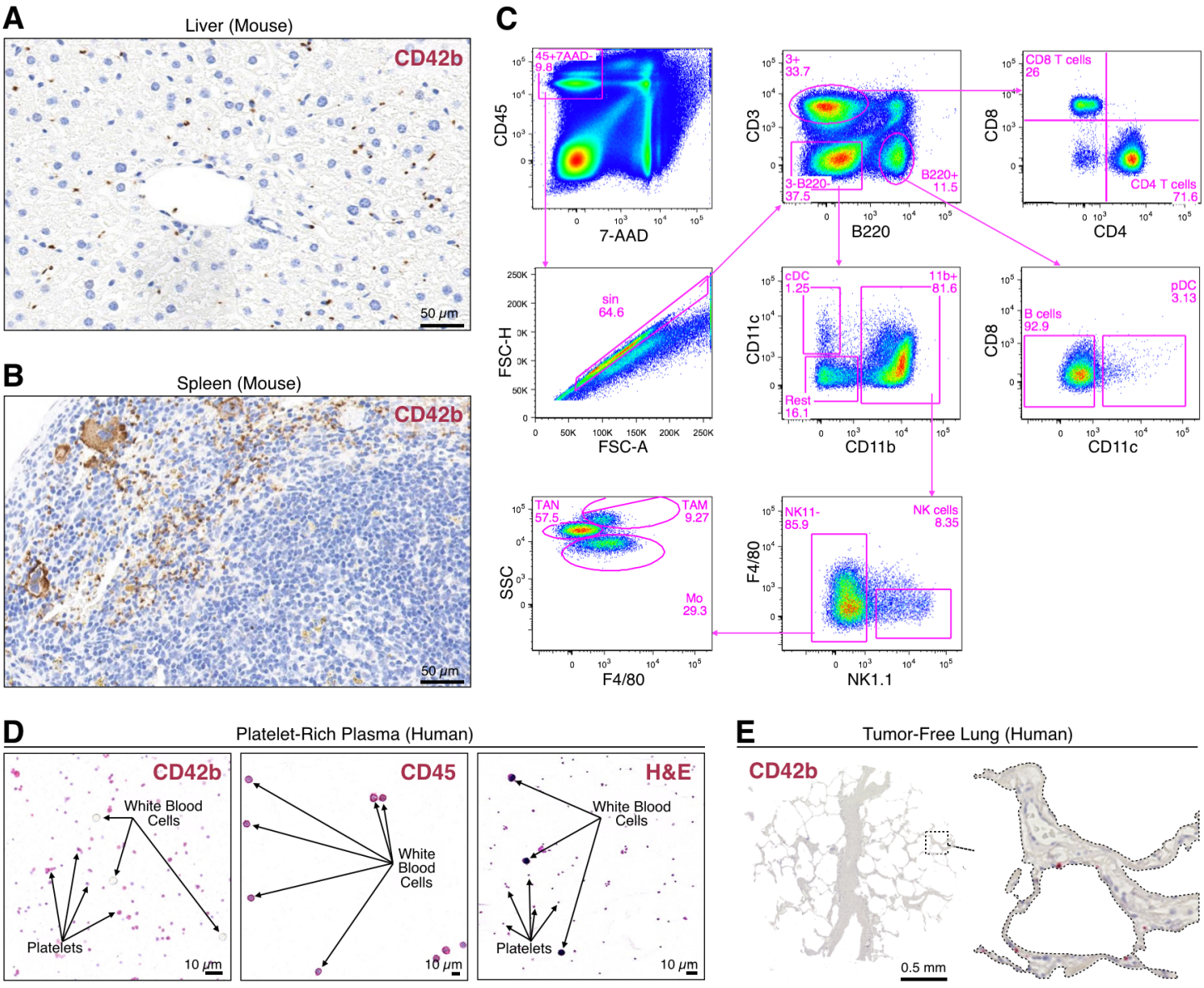

Figure S3. Related to Figure 3. Controls for staining platelets in murine and patient lung-tumor sections and for labeling murine tumor-infiltrating immune-cell subsets in flow-cytometry experiments.

(**A-B**) Immunohistochemistry staining for mCD42b (dark brown) on sections of liver (**A**) and spleen (**B**) from control mice. Scale bars represent 50 μm. Large megakaryocytes are visible in the subcapsular region of the spleen.

(**C**) Gating strategy used to quantify lung cell subsets in Fig 3C. Top left panel represent initial ungated plot. Sequential gating on regions is indicated by arrows.

(**D**) Immunohistochemistry staining for hCD42b (red, leftmost panel), hCD45 (red, middle panel) and hematoxylin and eosin (rightmost panel) on human platelet-rich plasma preparations.

(**E**) Immunohistochemistry staining for hCD42b (red) on lung cancer patient tissue microarrays. A representative example of non-involved, tumor-free tissue is shown.

Abbreviations are as follows: cDC, common dendritic cells; pDC, plasmacytoid dendritic cells; Mo, monocytes; NK, natural killer; sin, singlets; TAM, tumor-associated macrophages; TAN, tumor-associated neutrophils.

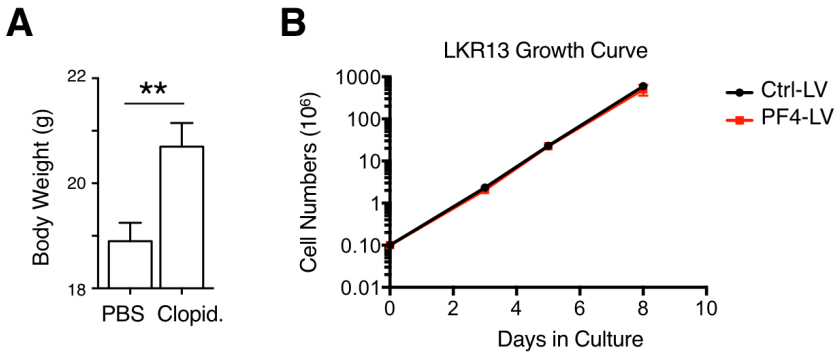

Figure S4. Related to Figure 4. Platelet-targeting agents influence cancer growth in a non-tumor cell autonomous manner.
(**A**) Body weight of PBS-treated and Clopidogrel-treated tumor-bearing mice 5 weeks after KP1.9 lung tumor cell injection (n=8-9).
(**B**) Growth curves of Kras lung-tumor cell line LKR13 transduced with either Ctrl- or PF4-LV.

Supplemental Experimental Procedures

Mice

Kras$^{LSL-G12D/+}$;*p53*$^{fl/fl}$ (referred to as KP) and *Kras*$^{LSL-G12D/+}$ (referred to as K) mice in a 129/j background were used as conditional mouse models of lung adenocarcinoma as described previously (Cortez-Retamozo et al., 2012). To induce lung adenocarcinoma, KP and K mice were infected with an adenovirus expressing Cre recombinase (AdCre) by intranasal instillation, as described previously (DuPage et al., 2009). AdCre was purchased from the University of Iowa Gene Transfer Vector Core. Control 129 mice were bought from The Jackson Laboratory. All animal experiments were approved by the Massachusetts General Hospital Subcommittee on Research Animal Care.

PF4 lentiviral vectors

Concentrated VSV.G-pseudotyped, third-generation LV stocks were produced and titered as described previously (De Palma and Naldini, 2002). Lentiviral vector copy per genome (CpG) was calculated by titering the concentrated LV on 293T cells. After 2 weeks in culture, we purified genomic DNA (Qiagen). Standard curve for LV quantification was obtained from transduced 293T cells sorted for carrying one CpG. The CpG of genomic DNA standard curves and samples was determined using custom TaqMan assays specific for LVs (Applied Biosystems). LVs were injected i.v. at $2 \bullet 10^4$ ng p24/mouse in 50-200 µl depending on the infectivity.

Real-time quantitative PCR analysis and statistical analysis

Tumor nodules were visually identified and resected. Nodules were lysed with a mechanical rotor in lysis buffer. Total mRNA was purified following RNeasy Mini kit guidelines (QIAGEN). RNA was quantified and retrotranscribed with High-Capacity cDNA Reverse Transcription Kit (Thermo Fisher). Quantitative PCR analyses were performed with TaqMan assays from Applied Biosystems. Quantitative PCR was run for 40 cycles in standard mode using a StepOne apparatus (Applied Biosystems). The SDS software was used to extract raw data. The difference between the threshold cycle (CT) of each gene and that of the endogenous control 18S (ΔCT) was used to determine gene expression. Statistical testing was performed on fold-change values using 2-way ANOVA followed by Holm-Sidak multiple comparison test. P values were considered significant when < 0.05.

ELISA

PF4 levels in the supernatant of total liver cells were quantified by ELISA kit (R&D Systems) following the kit guidelines.

Flow cytometry

Spleens and bone marrow were minced into single-cell suspensions by mechanical dissociation. Lung tumors were minced into single-cell suspensions by enzymatic treatment as previously described (Pucci et al., 2009). Cell suspensions were stained with directly-conjugated antibodies (from Biolegend, BD or eBiosciences) and 7AAD (Sigma). Cells of interest were identified as shown in Fig. S2C or Fig. S3A. Eleven-color analyses were performed on a custom LSRII (BD) equipped with: 405nm laser and, in order, 450/50, 505LP, 515/20, 600LP, 610/20, 685LP, 695/40 filters; 488nm laser and, in order, 488/10, 505LP, 530/30, 550LP, 575/26, 685LP, 695/40 filters; 633nm laser and, in order, 660/20, 710LP, 730/45, 735LP, 780/60. Fluorochromes employed were, in order: BV421 or eFluor450, BV510, BV605, BV711, FITC or eGFP or eYFP, PE, 7AAD or PerCP-Cy5.5, PE-Cy7, APC, Alexa700, APC-Cy7 or APC-eFluor780.

Mouse Histology and Immunohistochemistry

For histological analysis of tumor burden in mice, lung tissues were harvested, formaldehyde-fixed and paraffin-embedded following standard procedures. Consecutive sections were prepared and stained with hematoxylin and eosin to define tumor tissue areas in the lung. Immunohistochemistry (IHC) on mouse tissue sections was performed as described previously (Pfirschke C, 2016). Briefly, mouse lung tumor sections were prepared and dried at 60°C for 1 h, dewaxed and rehydrated. We performed heat-induced epitope retrieval by incubating in 10 mM Tris (pH9.0) buffered solutions containing 0.05% Tween heated at 120°C for 2 min. To obtain consistent and reliable staining an automated staining system (LabVision Autostainer 360, Thermo Scientific) was used. To destroy all

endogenous peroxidase and alkaline phosphatase activity in the tissue, the sections were pretreated using BLOXALL endogenous enzyme-blocking solution (Vector Laboratories) for 10 min. After a blocking step with normal goat serum, the sections were incubated with the individual primary monoclonal antibody (mAb) for 1 h followed by secondary ImmPRESS polymer detection systems (Vector Laboratories) according to the manufacturers protocol. The DAB Plus Substrate System (Thermo Scientific) was applied as substrate and hematoxylin used for counterstain. Rat anti-mouse CD42b (clone Xia.G7, emfret Analytics) was used for staining mouse lung tumors and control tissues. Image documentation was performed using the NanoZoomer 2.0-RS slide scanner system (Hamamatsu) and CD42b positivity was identified using Fiji software.

Human Tumor Samples and Immunohistochemistry

Sections from paraffin-embedded biopsies of lung resections (n=29) from lung adenocarcinoma patients with known *KRAS* gene mutation status were obtained from the Department of Pathology at Massachusetts General Hospital. TP53 IHC was conducted with mAb clone DO-7 (Leica) as described previously (Pfirschke C, 2016). The following scoring system was used to assess *TP53* wild-type or mutational status (Köbel et al., 2010): score 0 (complete absence of staining: *TP53* null mutation); score 1 (focal nuclear expression in up to 50% of tumor cells: *TP53* wild-type); score 2 (nuclear overexpression in more than 50% of tumor cells: *TP53* missense mutation). Biopsies with scores 0 or 2 were categorized as *TP53* mutants and biopsies with score 1 as *TP53* wild-type. CD42b IHC was performed with an anti-human CD42b mAb (clone 42C01, Abcam) and CD42b positivity was identified using Fiji software.

Platelet-rich plasma (PRP) preparation and staining

PRP smears were analyzed to assess the specificity of the anti-human CD42b mAb (clone 42C01, Abcam). Human blood was collected in a vacuum tube containing anticoagulant and blood was centrifuged at 300 g for 15 min. Following centrifugation, 10 µl of the upper fraction, containing the PRP, was applied on a clean glass slide and a thin smear was prepared. After drying for 1 h the PRP smear was fixed in 4% formaldehyde-buffered solution and IHC performed as described above, omitting the heat-induced epitope retrieval. In addition, control staining with anti-human CD45 mAb (clone 2B11+PD7/26, DAKO) was performed to confirm that PRP was indeed depleted of leukocytes and to demonstrate the specificity of the CD42b mAb, which does not stain CD45+ leukocytes but only platelets.

Clopidogrel Treatment

Platelet inhibition was performed by daily i.p. injections of 10 mg/kg Clopidogrel (Quinn and Fitzgerald, 1999). Treatment was initiated 2 days before tumor challenge and for a duration of 5 weeks. KP1.9 cells ($2.5 \bullet 10^5$) were injected i.v.

Bioinformatics and Statistics

In silico analyses were performed in R. The initial list of murine candidates (i) used to probe lung cancer patient microarray datasets (ii) was sequentially transformed from a list of murine proteins into: 1) their human orthologs; 2) their gene symbol; 3) the corresponding microarray probe IDs. The list of microarray probes was then matched with human datasets for survival analysis, which used the log-rank test with Bonferroni correction. Such survival analysis consisted to operationally sort patients according to expression levels of each of the candidates, select high and low expressing patients (top and bottom 20%) and compare their overall survival. Unless otherwise specified, results were expressed as mean ± SEM. GraphPad Prism 6 was used for all statistical analyses. Statistical tests for multivariate analyses were performed using 2-way ANOVA followed by Holm-Sidak multiple comparison test. P values were considered significant when < 0.05.

Supplemental References

Cortez-Retamozo, V., Etzrodt, M., Newton, A., Rauch, P.J., Chudnovskiy, A., Berger, C., Ryan, R.J., Iwamoto, Y., Marinelli, B., Gorbatov, R., Forghani, R., Novobrantseva, T.I., Koteliansky, V., Figueiredo, J.L., Chen, J.W., Anderson, D.G., Nahrendorf, M., Swirski, F.K., Weissleder, R., and Pittet, M.J. (2012). Origins of tumor-associated macrophages and neutrophils. Proc Natl Acad Sci U S A *109*, 2491–2496.

De Palma, M., and Naldini, L. (2002). Transduction of a gene expression cassette using advanced generation lentiviral vectors. Methods Enzymol *346*, 514–529.

DuPage, M., Dooley, A.L., and Jacks, T. (2009). Conditional mouse lung cancer models using adenoviral or lentiviral delivery of Cre recombinase. Nat Protoc *4*, 1064–1072.

Köbel, M., Reuss, A., du Bois, A., Kommoss, S., Kommoss, F., Gao, D., Kalloger, S.E., Huntsman, D.G., and Gilks, C.B. (2010). The biological and clinical value of p53 expression in pelvic high-grade serous carcinomas. J Pathol *222*, 191–198.

Nguyen, D.X., Chiang, A.C., Zhang, X.H., Kim, J.Y., Kris, M.G., Ladanyi, M., Gerald, W.L., and Massagué, J. (2009). WNT/TCF signaling through LEF1 and HOXB9 mediates lung adenocarcinoma metastasis. Cell *138*, 51–62.

Pfirschke C, E.C., Rickelt S, Cortez-Retamozo V, Garris C, Pucci F, Yamazaki T, Poirier-Colame V, Newton A, Redouane Y, Lin YJ, Wojtkiewicz G, Iwamoto Y, Mino-Kenudson M, Huynh TG, Hynes RO, Freeman GJ, Kroemer G, Zitvogel L, Weissleder R, Pittet MJ (2016). Immunogenic Chemotherapy Sensitizes Tumors to Checkpoint Blockade Therapy. Immunity *44*, p343–p354.

Pucci, F., Venneri, M.A., Biziato, D., Nonis, A., Moi, D., Sica, A., Di Serio, C., Naldini, L., and De Palma, M. (2009). A distinguishing gene signature shared by tumor-infiltrating Tie2-expressing monocytes, blood “resident” monocytes, and embryonic macrophages suggests common functions and developmental relationships. Blood *114*, 901–914.

Quinn, M.J., and Fitzgerald, D.J. (1999). Ticlopidine and clopidogrel. Circulation 100, 1667–1672

Taguchi, A., Politi, K., Pitteri, S.J., Lockwood, W.W., Faca, V.M., Kelly-Spratt, K., Wong, C.H., Zhang, Q., Chin, A., Park, K.S., Goodman, G., Gazdar, A.F., Sage, J., Dinulescu, D.M., Kucherlapati, R., Depinho, R.A., Kemp, C.J., Varmus, H.E., and Hanash, S.M. (2011). Lung cancer signatures in plasma based on proteome profiling of mouse tumor models. Cancer Cell *20*, 289–299.